Research on Performance Optimization of Arched Transfer Beams in a Complex Office Building

Wenjun Jing*, Han Ji, Zhuohang Zhang, Wei Zhang, Mengyao Miao, Qian Yu

Central-South Architectural Design Institute Co, Ltd, Wuhan, Hubei, 430000, China

*jingwenjun6010@csadi.cn

Abstract. To enhance the application of arch-shaped beams in public buildings, this article utilizes ABAQUS and engineering design software to analyze the impact of different structural measures on the stress performance of a high-rise building's large-span cast-in-place reinforced concrete arch conversion beam.

Four structural models are constructed: a pure RC arch beam-column, an arch steel beam-column, an arch steel beam-column with internal steel support, and a rectangular steel beam-column with steel support. These models are systematically analyzed to assess stress conditions under various structural conditions.

The research reveals that the concrete arch beam exhibits a significant arch effect, resulting in a distinct force transfer path compared to conventional RC beams. This characteristic poses challenges for traditional engineering design software to accurately capture and calculate stress states.

To address this, a "hollow honeycomb" concrete construction measure is adopted at the arch foot of the framed arch beam, reducing self-weight and conserving concrete usage. Additionally, steel supports are emphasized to be placed in critical areas of the pressure arch transfer path to maximize their support function and enhance structural stress performance.

Keywords: Arched beams; Steel support; Finite element analysis; Arch effect

1   Introduction

Currently, the reinforced concrete arch structure in China finds extensive utilization primarily in bridge construction. This structural format boasts robust carrying capacity, cost-effective nature, and aesthetically pleasing appearance [1]. Notably, the fasting arch structure exhibits superior theoretical control over vertical stiffness and long-term deflection deformation compared to traditional PC continuous rigid bridges [2].

To cater to the aesthetic demands of large-span and high-clearance public buildings, steel frames or steel-concrete composite structures prevail, while the application of arch structures remains limited. This is due to the intricate nature of arch beams, which surpass rectangular beams in complexity, making it challenging for standard engineering design software to simulate the arch structure accurately.

Therefore, we focus on the large-span cast-in-place reinforced concrete arch conversion beam of a high-rise building and utilize the ABAQUS general finite element

analysis software to delve into various structural forms of conversion beams. Furthermore, we evaluate the stress characteristics of arched structural beams under the limiting state of bearing capacity. This comprehensive study aims to provide valuable insights and serve as a reference for the application of arch structures in the realm of public buildings.

2   Project Overview

The project, situated in Yubei District of Chongqing, comprises a pair of seven-story office buildings above ground, flanked by a two-story basement. The designated service life of the main structural components is stipulated to be fifty years, adhering to a structural safety grade of II. The seismic fortification intensity is set at six degrees, with a designated basic seismic acceleration of 0.05g. The project falls under seismic grouping I and is categorized as a class III site, with a soil characteristic period of Tg=0.45s. Furthermore, the seismic fortification category is designated as quasi-fortification, specifically Class C. The structural characteristics of the project can be summarized as follows: (1) The building's design includes penetrating columns, multiple towers, and interconnected buildings, classifying it as vertically irregular and non-standard. Local floor areas have compromised connections due to arities.(2) Numerous extended overhangs within the plane pose earthquake resistance challenges. Vertically, cantilevered supporting column transfers and large-span structures compromise vertical force transmission efficiency.(3) Site topography varies, with the northern basement subterranean and the southern section exposed. Structural design considers B1 as the embedded level and the underground first floor as the podium.(4) Considering local fabrication, construction cycle, and other factors, the superstructure above the transfer floor adopts a steel framework. This study focuses on South Tower 1.

The design requirements for the second-floor transfer beam are: (1) uphold architectural curvature, ensuring structural integrity and aesthetic appeal; (2) use inclined rods to connect transfer beam and column for effective load distribution and stability[3]; (3) securely connect modified side column base with a concealed beam for bidirectional restraint and structural rigidity.

Current general design software lacks the ability to simulate the unique arch-shaped structural beam. Therefore, this project proposes a design solution: a rectangular steel reinforced concrete beam with an arch-shaped thin concrete plate beneath to create a cavity and achieve the desired architectural form. A concealed box-type diagonal brace is placed at the beam-column joint, as shown in Figure 2.To evaluate five structural configurations, this study utilizes YJK software to establish structural models for each. Internal forces are extracted considering 1.3 and 1.5 factors for dead and live loads, respectively. Detailed finite element models are constructed using ABAQUS software for a thorough stress analysis under basic working conditions.
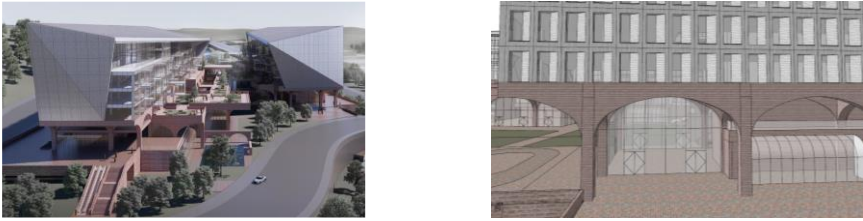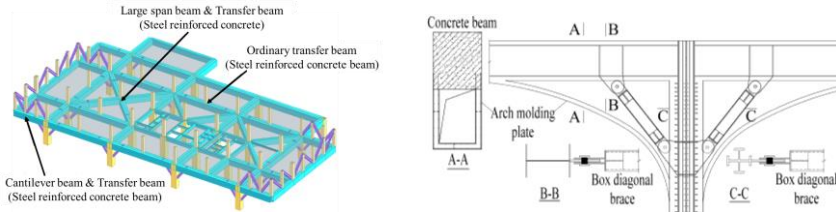
Fig. 1. Overall effect drawing of building

Fig. 2. Detailed drawing of arch node

3   Finite Element Model

3.1   Model Establishment

To analyze the local structure of the second-floor transfer floor, the dimensions of the column are 1200×1200 mm, encompassing a cross-sectional steel element with dimensions of $600 \times 250 \times 40$ mm. The beam measures 1200×1400 mm, containing I-shaped steel ribs of dimensions $1100 \times 600 \times 18 \times 25$ mm. The column stands at a height of 12 m, while the cantilever beam spans 8.25 m, the middle beam spans 15.6 m, and the inner radius of the arch beam is 12.3 m. Five refined finite element models, designated as Model1-5 (hereinafter referred to as M1-5), have been established using the ABAQUS software package, as depicted in Figure 3.
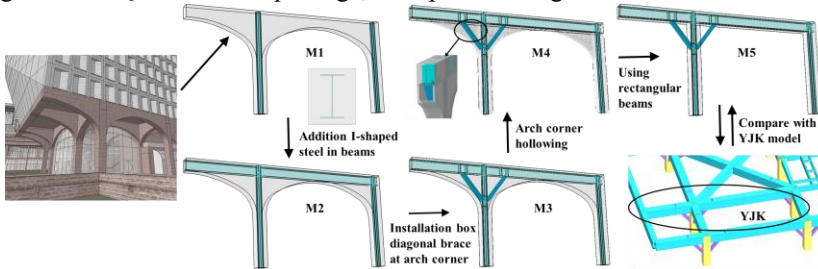

Fig. 3. Finite element model

M1 is a robust reinforced concrete arch structure. M2 builds upon M1 by incorporating I-shaped steel ribs within the arch beam. M3 further enhances M2 by incorporating $600 \times 400 \times 25$ mm and $500 \times 400 \times 16$ mm box-shaped diagonal braces at the

arch foot. Based on the M3 structure, M4 hollows out the interior concrete of the concrete arch, creating a cavity within the arch to reduce concrete volume while ensuring the isolation of the box-shaped diagonal brace from the arch concrete. Finally, M5 represents a simplified variant of M4, where during calculations, the arch beam is approximated as a rectangular beam, and diagonal braces are positioned at the beam-column junctions, disregarding the influence of arched thin plates. This approach aligns with the YJK model utilized in the design software.

The C3D8R solid element serves as a modeling tool for representing concrete components and steel skeletons. Within this framework, the mesh size is specifically tailored for concrete, measuring 300 mm, while the steel mesh size is set to 100 mm to ensure precision. Furthermore, the internal reinforcement structure is accurately simulated using linear beam elements, adopting a grid size of 100 mm. Additionally, the steel diagonal brace is simulated through the utilization of linear beam elements, maintaining a consistent grid size of 100 mm.

3.2   Material Model

The Concrete Damaged Plasticity module in ABAQUS software serves as a robust tool for simulating the constitutive behavior of concrete materials. This approach comprehensively accounts for material damage and crack propagation characteristics under loading conditions. By introducing two independent parameters representing compression and tension damage factors, it effectively captures the dual failure mechanisms inherent in concrete: compressive crushing and tensile cracking[4].

The output data generated from this model, namely Compressive Damage and Tension Damage results, facilitate detailed analyses of the extent of cracking within concrete structures during bending resistance and shear actions. This information is invaluable in assessing the structural integrity and performance of concrete components.The stress-strain relationship of concrete materials is rigorously defined in accordance with the Code for Design of Concrete Structures (GB50010-2010)[5], ensuring compliance with industry standards and best practices. Furthermore, the damage factor for concrete is calculated using a damage formula derived from the Sidoroff energy equivalence principle, a well-established theoretical framework in material science[6]. For simulating the behavior of steel, a trilinear material model incorporating a yield phase and a linear reinforcement phase is employed. This model enhances the ideal elastoplastic material model by introducing a reinforcement phase once the steel attains its yield strength, thereby providing a more realistic representation of steel's structural response[7-9].

3.3   Material Properties

The structure, constructed with C40 concrete, possesses a modulus of elasticity amounting to 3.25×10^4 MPa and exhibits a Poisson's ratio of 0.2. Furthermore, the internal reinforcement and diagonal bracing components of this concrete structure are comprised of Q355B steel, boasting a modulus of elasticity reaching 2.06×10^5 MPa and maintaining a Poisson's ratio of 0.3. Additionally, the longitudinal reinforcement

and hoop reinforcement, both of which contribute significantly to the overall structural integrity, are fabricated from HRB400 steel, displaying a modulus of elasticity identical to that of the Q355B steel, specifically 2.06×10^5 MPa, and a Poisson's ratio consistent with the former, being 0.3.

3.4   Boundary Conditions and Calculated Loads

The ABAQUS model simulates consolidation by imposing constraints at the column bottom, specifically UX, UY, UZ, URX, URY, and URZ, while limiting lateral displacement and torsion out of plane by applying constraints at the column top, namely UX, UZ, URX, and URY. The loads incorporated into the model primarily consist of structural self-weight, uniform floor loading, loads transferred from the beam, and loads transmitted from the upper column. Based on the computational outcomes of the YJK model, the forces acting on each node under the combined condition of 1.3 times the dead load and 1.5 times the live load have been extracted. Subsequently, the vertical forces and bending moments are imposed onto the designated loading points 1 through 4, as depicted in Figure 4.

Upon completion of the calculations, it is determined that the seismic action of the selected representative frame falls within a non-controlling operational scenario. Therefore, only in-plane bending moments and vertical loads are taken into account. The specific loads allocated to each loading point are detailed in Table 1.
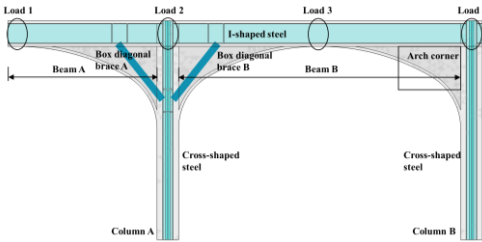

Fig. 4. Diagram of the model

Table 1. Load parameters

Loading position	Vertical force(kN)	Bending moment (kN×m)
1	2899.7	6104.8
2	10525.1	-1741.9
3	5123.2	-332.1
4	8111.0	2441.6

3.5   Model Calculation Results

Based on the calculations performed for M1~5, the vertical displacement data for points 1~6 located at the beam's top have been extracted and subsequently compared with the corresponding values obtained from the YJK model. It is noteworthy that, due to the constraint imposed by the ABAQUS model on the displacement at the column's base, it is necessary to adjust the vertical displacement values at the beam's top in the YJK model, taking into account the vertical displacement at the column's base. The comprehensive comparison outcomes are presented in Figure 5, which offers a visual representation of the disparities. Additionally, a comparative analysis of the axial forces exerted by diagonal braces A and B is detailed in Table 2, providing a quantitative assessment of their performance.
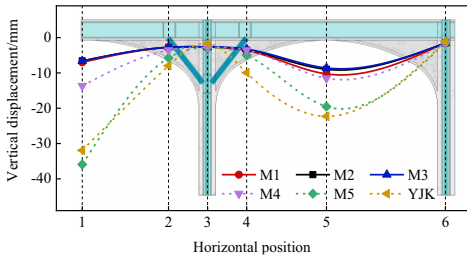
Fig.5.ertical change curve of the beam top

Table2. Axial force of diagonal brace

Model	Diagonal brace A (MPa)	Diagonal brace B (MPa)
YJK	-126.97	-152.4
M3	-25.02	-26.63
M4	-50.74	-58.95
M5	-122.73	-144.09

After a thorough comparison between Model 5 and YJK, it has been observed that there exists a negligible disparity in terms of vertical displacement, while a consistent pattern of deformation is evident. This finding indicates a close congruency in the beam deflection calculations, staying within the stipulated structural capacity limits.

A granular analysis of individual models reveals that cantilever beams A and B exhibit deflections that fall well within the permissible limit values. Notably, in models ranging from M1 to M3, the deflection magnitudes of these beams are significantly mitigated due to the incorporation of a solid concrete arch structure.

However, a notable deviation is discernible between the results obtained from Model M4 and YJK. This discrepancy can be attributed to the strategic placement of concrete at the arch angle of M4, which effectively reduces cantilever beam deflections and diagonal brace stress.

In the event that Model M5 is selected for implementation, utmost caution must be exercised during the construction phase. It is imperative to avoid integral pouring of the concrete thin plate and beam-column connections to ensure structural integrity. Additionally, construction should commence only after the beam-column shrinkage, creep, and minor deformation of the supporting structure have stabilized, to guarantee the safety and durability of the final structure.

4   Comparative Study on Structural Stress Characteristics

4.1   Comparative Stress Study of Concrete Structures

Under basic conditions,the longitudinal stress distribution of M1~5 concrete structure is shown in Fig.6.

The results indicate congruency in longitudinal stress among M1 to M5 concrete structures. Significant compressive stresses are observed at the top of B span beam, while tensile stresses are present at the top of column A and bottom of B span beam. Comparison of M1 to M3 shows reduced internal forces in concrete arch structure with section steel and diagonal braces. Tensile stress at the top of beam in M1 to M4 is smaller than in M5 rectangular beam. The longitudinal stress range in the compression area of the arch at cantilever beam A is -8.27 to -0.19, -7.82 to -1.07, -7.89 to -0.73, and -18.88 to -1.47 MPa (negative values represent compressive stress).
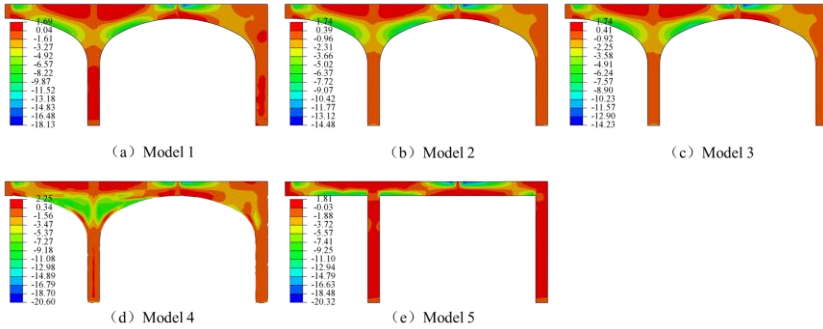
(a) Model 1   (b) Model 2   (c) Model 3

(d) Model 4   (e) Model 5

Fig.6. Longitudinal stress distribution of concrete(MPa)

Upon examination of the axial forces exerted by the diagonal braces specified in Table 2, it is evident that the utilization of the arch structure within the beam results in the concrete located at the primary load-bearing position of the beam-column joint being situated at the arch corner. Consequently, the diagonal braces fail to fully demonstrate their intended performance. In the case of M3, when the diagonal brace is positioned within the concrete, it may be subjected to bending moments arising from concrete deformation, which is detrimental to the structural integrity and force transmission capabilities of the diagonal brace.Comparatively, the hollow-out design of the arch corner in M4 serves to mitigate internal stress within the beam and enhance the efficiency of force transmission through the diagonal brace. However, it must be noted that the efficiency achieved by this design is inferior to that of the diagonal brace employed in M5. Although the internal forces exhibited by M4 are notably lower than those of M5, the presence of numerous edges and sharp corners within the hollowed-out areas results in an uneven distribution of internal forces and a concentration of stress.Regarding the longitudinal stress profile of M5 concrete, it is observed that in the majority of regions, the stress ranges from -16.63 MPa to 1.81 MPa. This indicates a generally low level of compressive stress, with ample margin relative to the standard values prescribed for concrete. Additionally, there are instances where a slight tensile stress phenomenon is evident within the concrete.
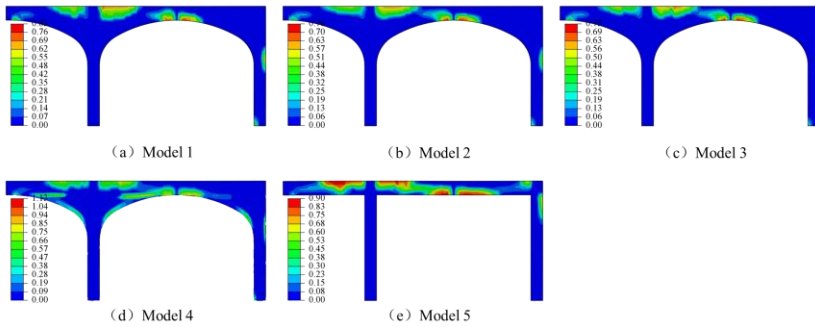

(a) Model 1   (b) Model 2   (c) Model 3

(d) Model 4   (e) Model 5

Fig.7. Distribution of tension damage in concrete

The distribution of DAMAGET can be used to analyze the degree of damage of concrete under tension.The damage range is 0-1(0 means no damage,1 means complete damage).The distribution of tension damage of M1~5 concrete beam is shown in Fig.7.

Fig.7 shows that the solid arch structure of M1~3 has less tension damage than that of M4 and M5.M1~3 reduces damage of concrete arch by setting section steel and diagonal brace,and the effect of section steel is more obvious.The top tension damage of M4 is significantly lower than that of M5,but there is a sudden change of damage at individual locations.The damage values of M5 at the top of column A and the bottom of beam B span reach above 0.8,and there is more serious tension damage.Combined with Fig.6,it can be seen that the tension stress of concrete in this area is too high and cracks may occur.However,due to the existence of steel bars and I-shaped steel,when slight cracks occur in concrete structure under tension,the tension force is mainly borne by steel members.

4.2   Comparative Stress Study of Beam Sections

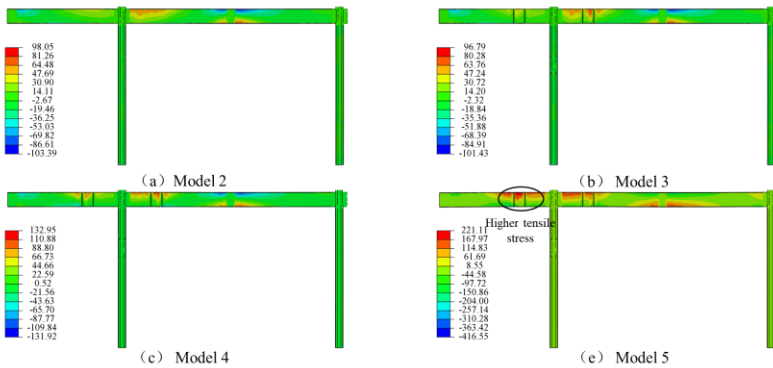Under basic conditions,the longitudinal stress distribution of M2~5 I-shaped steel is shown in Fig.8.

Fig.8. Longitudinal stress distribution of I-shaped steel(MPa)

Figure 8 show alignment of I-shaped steel tension zone with concrete structure, resulting in uniform stress. Section steel in M2-M5 beams exhibits consistent longitudinal stress trends. Minor stress differences in M2 and M3 suggest minimal impact from diagonal braces. M4 steel contributes more to internal forces than M3. M5 exhibits significant tension at cantilever beam A's top, indicating arch structure's effectiveness. Steel in M5 ranges from -97.72 to 167.97 MPa, peaking at 221.11 MPa, effectively absorbing tension and minimizing concrete cracking. Steel usage in M2-M4 is less efficient. Arch beam structure allows for reduced I-shaped steel section size, enhancing concrete-steel synergy.

4.3   Comparisons of Longitudinal Bar Stresses at The Beam Top

Under basic conditions,the longitudinal stress distribution of top longitudinal reinforcement of M1~5 beam is shown in Fig.9.Upon comparing M1 and M2, the installation of I-shaped steel in the beam significantly reduced tension stress on the top surface. Minor differences in primary stress ranges between M2 and M3 indicate minimal impact from the diagonal brace in the arch structure. In contrast, reinforcement internal forces in M4 increased, enhancing service efficiency. For M5, the longitudinal reinforcement's stress range spans from -160.52 MPa to 297.32 MPa, elevated compared to other structures, improving efficiency. Stress levels remain below yield strength, ensuring safety. The rectangular concrete steel frame beam in M5 facilitates efficient construction with uniform stress distribution and smoother internal force transfer. The design incorporates reduced stiffness and box diagonal braces, resulting in a ductile system with strong columns and weak beams, advantageous for seismic design.
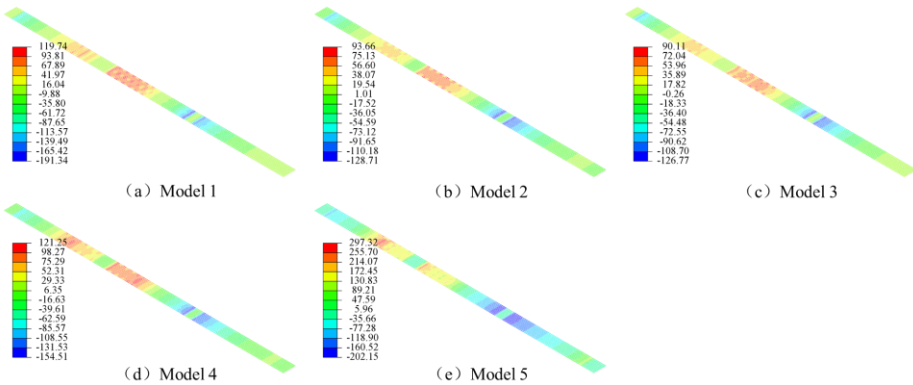

（a）Model 1   （b）Model 2   （c）Model 3

（d）Model 4   （e）Model 5

Fig.9. Longitudinal stress distribution of longitudinal reinforcement at the beam top(MPa)

5   Conclusion

This paper delves into the intricate finite element models of various beam structures within an office building, serving as the focal point of our investigation. Through rigorous analysis, a comparative examination is conducted regarding the stress states of newly conceived structural designs and their diverse structural configurations under baseline conditions. The findings of this meticulous study reveal that:

(1)   The arch structure effectively reduces deflection and internal force. In cantilever arch structures, the beam roof experiences significant tensile stress. Steel bones and inclined supports are crucial in arch structures, with steel bones having a greater impact.

(2)   Compared with solid arch structure, hollow design reduces internal stress of the beam and enhances force transmission efficiency of inclined support. However,

stress concentration and damage mutation occur in some positions. Chamfer strengthening measures are recommended for angular areas in engineering applications.

(3)   The structural form of hollow arch Angle + inner storage steel support M4 in the rectangular concrete beam, the steel bone and steel bar bear the tensile well, thus limiting the continuous cracking of concrete.

(4)   The structure form of arch angle hollow out + inner steel support M4 is convenient. Compared to the arch beam, it efficiently utilizes steel strength, improving inclined support efficiency. Stress distribution is uniform, reducing beam stiffness and creating a strong column-weak beam system, enhancing earthquake resistance.

(5)   Arched structural beams are suitable for public buildings, fulfilling bearing capacity needs while preserving facade shape and enhancing building span. Future studies can explore seismic performance of node positions through dynamic analysis of arched beam-column connections.

References

1. Yin K C,Yuan J,Yi Z Y,et al.(2023)Design of Arch Beam Combination Section of Long Span Through Arch Bridge.Value Engineering,42(20):91-93.DOI:10.3969/j.issn.1006-4311.2023.20.029.
2. Lai Y P,Wang G N,Yan F C,et al.(2023)Design theory and method for long-span arch-stiffened girder rigid-frame bridge China Civil Engineering Journal,56(09):65-80.DOI:10.15951/j.tmgcxb.22050442.
3. Tan Q,Luo X F,Xu X P,et al.(2022)Design and analysis of complex steel structure on slopes of Chongqing Liang Jiang Coordinated Planning Exhibition Center.Building Structure,52(08):8-15+7.DOI:10.19701/j.jzjg.20211449.
4. Zhang Z H,(2022).Mechanical behavior of steel-concrete joint section with no cells and rear bearing plates.DOI:10.27466/d.cnki.gzzdu.2022.003672.
5. General Administration of Quality Supervision,Inspection and Quarantine,(2010)GB 50010-2010,Code for design of concrete structures.
6. Tahmasebinia F A,Ranzi G A,Zona A B.(2013)Probabilistic three-dimensional finite element study on composite beams with steel trapezoidal decking(Article).Journal of Constructional Steel Research,80:394-411.
7. General Administration of Quality Supervision,Inspection and Quarantine,(2017)GB 50017-2017,Standard for design steel structures.
8. Wang X L.(2019)Experimental and theoretical study on bearing capacity of steel-concrete composite beams.DOI：10.27135/d.cnki.ghudu.2019.002295.
9. European Standard CEN,(2005)EN 1993-1-5.Eurocode 3-Design of steel structures-Part 1-5:Plated structural elements.